

One-step methyl isobutyl ketone (MIBK) synthesis from 2-propanol: Catalyst and reaction condition optimization

G. Torres, C.R. Apesteguía, J.I. Di Cosimo*

GICIC (Catalysis Science and Engineering Research Group), INCAPE (UNL-CONICET), Santiago del Estero 2654, 3000 Santa Fe, Argentina

Received 3 August 2006; received in revised form 3 October 2006; accepted 8 October 2006

Available online 17 November 2006

Abstract

A gas-phase process for methyl isobutyl ketone (MIBK) synthesis from 2-propanol in one-pot is studied as an alternative to the conventional technology for producing MIBK from acetone (DMK). Bifunctional copper/acid–base catalysts able to operate at mild temperatures and atmospheric pressure were prepared and characterized by measuring the acid and base properties as well as the metal dispersion. It was found that a Cu–Mg–Al mixed oxide catalyst gives high MIBK yields. In this catalyst, the metal fraction in loadings of 2–6 wt% promotes the hydrodehydrogenation steps at high rates whereas the surface acid–base sites of moderate acid and base properties favor the aldol condensation reaction.

The effect of different operational conditions such as reaction temperature and reactant partial pressure was also investigated. The MIBK formation rate was enhanced by increasing 2-propanol partial pressure in a wide range, consistently with a positive 2-propanol reaction order in the overall kinetics whereas the presence of hydrogen in the reactant mixture inhibited MIBK synthesis due to a negative order with respect to H₂. An increase of the reaction temperature and the use of inert atmosphere improved the MIBK yield. By operation at 533 K in N₂ the Cu–Mg–Al catalyst with 6.4 wt% Cu, yields 27% MIBK in comparison to the 30% typically obtained in current commercial liquid-phase high-pressure processes from DMK.

© 2006 Elsevier B.V. All rights reserved.

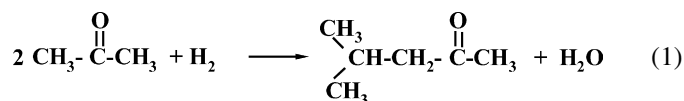
Keywords: Methyl isobutyl ketone (MIBK); 2-Propanol; Aldol condensation; Bifunctional catalysis

1. Introduction

4-Methyl-2-pentanone, methyl isobutyl ketone (MIBK), acetone (DMK) and methyl ethyl ketone are the aliphatic ketones most produced worldwide. In particular, MIBK is widely used as a solvent for vinyl, epoxy and acrylic resin production as well as for dyes and nitrocellulose. MIBK is also employed as an extracting agent for antibiotic production or removal of paraffins from mineral oils, in the synthesis of rubber chemicals, and in fine chemistry applications [1,2]. The global demand for MIBK is estimated in 300,000 t per year.

Nowadays, MIBK is industrially obtained in a one-step liquid-phase process from DMK and H₂ at low temperatures (393–433 K) and high pressures (1–10 MPa) in multitubular fixed bed reactors. The chemical reaction for this process is

depicted in Eq. (1).



Several reaction steps are comprised in Eq. (1): (i) aldol condensation of DMK to diacetone alcohol; (ii) dehydration of diacetone alcohol to mesityl oxide (MO); (iii) hydrogenation of the C=C bond of MO to MIBK. Therefore, multifunctional catalysts such as Pd or Pt supported on sulfonated resins, which contain condensation, dehydration and hydrogenation functions are used in the industrial process [1,3]. Both the aldol condensation and the dehydration reactions are reversible at 393–433 K [3] but the catalyst shifts the equilibrium in favor of MO by irreversibly hydrogenating it to MIBK [4].

In the commercial process, DMK conversion is typically 30–40% and the selectivity to MIBK reaches 90%. Thus, MIBK concentration in the reactor effluent before distillation is

* Corresponding author.

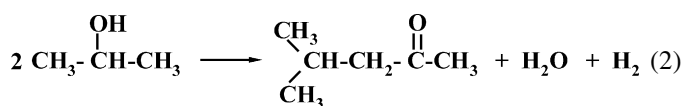
E-mail address: dicosimo@fiqus.unl.edu.ar (J.I. Di Cosimo).

usually lower than 30 wt%. In addition to the MIBK purification cost, the process requires high pressures to operate efficiently.

There is therefore a great interest for developing novel one-step processes able to operate at atmospheric pressure with comparable or better MIBK yields. Recently, Talwalkar and Mahajani [5] summarized conversion and selectivity of the most promising catalysts reported in the literature for MIBK synthesis from DMK at atmospheric or high pressures. Group VIII or IB metals such as Pd, Pt, Ni and Cu on acidic or basic supports like aluminosilicates, zeolites, mixed oxides and ion exchange resins are mostly postulated. In particular, Pd [4,6–8] or Ni [9,10] supported on Mg–Al or Zr–Cr mixed oxides, alumina, HZSM5, Cu/MgO [11] and Cu–Mg alloy powders [12] are reported to provide, in gas-phase and atmospheric pressure, MIBK yields similar or higher than that of the industrial process. However, none of these catalysts have been commercially implemented and there are no industrial plants operating in the gas-phase at atmospheric pressure.

The DMK used as reactant in the current commercial process must be obtained from other sources in a separate reactor. The main DMK manufacturing processes are: (i) Wacker–Hoechst direct oxidation of propane; (ii) dehydrogenation of 2-propanol; (iii) co-product of the phenol synthesis by the Hock process. The most important route worldwide is the Hock process followed in Western Europe, USA and Latin America by the dehydrogenation of 2-propanol [13]. In the latter process, DMK is synthesized from 2-propanol in fixed bed reactors at 493–573 K on Cu-based catalysts [1]. In MIBK manufacturing plants using this technology, the unreacted 2-propanol is then recycled, and hydrogen and DMK are stripped from the product mixture and sent to the MIBK synthesis unit. However, DMK must be previously purified and cooled down, thus increasing the operating cost of the MIBK synthesis.

Several attempts have been reported on the direct ketone synthesis from alcohols. In 1936, Dupont patented a one-step ketone synthesis process from secondary alcohols, in which MIBK was obtained with a 21 wt% yield on a copper-based catalyst at 600–633 K and 100–700 kPa [14]. Other pioneering works can be found in references [15,16]. In a previous work [17], we postulated a gas-phase process for the synthesis of MIBK in one-step at mild temperatures and atmospheric pressure using 2-propanol as reactant. This process is intended to be used in solvent manufacturing plants where producing a mixture of DMK, MIBK and other higher oxygenates would present high commercial interest. The overall reaction for this synthesis process is represented in Eq. (2):



Main consecutive reactions involved in the reaction network from 2-propanol are: (i) dehydrogenation of 2-propanol; (ii)

self-condensation of DMK to the α,β -unsaturated intermediate, MO; (iii) hydrogenation of the C=C bond of MO to MIBK.

This direct process from 2-propanol presents several technical advantages, such as to overcome the unfavorable thermodynamics of the MIBK synthesis from DMK, that must be carried out at low temperatures and high pressures and forms concomitantly significant amounts of 2-propanol. Furthermore, 2-propanol is commonly used in fine chemistry as a source of hydrogen for the gas-phase reduction of unsaturated ketones or aldehydes [18–20]. This hydrogen donor capacity of 2-propanol allows to carry out the MIBK synthesis from 2-propanol without supplying gas-phase hydrogen.

In this paper, we continue our investigations on the MIBK synthesis from 2-propanol using bifunctional catalysts that combine in intimate contact a metallic function needed for the hydro-dehydrogenation steps with an acid–base site required by the aldol condensation reaction. We have prepared and characterized several Cu-based catalysts with different copper loadings and acid–base properties and we have compared their catalytic performance. In addition, we investigated the effect of the operational variables such as reaction temperature on the catalyst activity and stability and MIBK yield. We also studied the effect of varying the 2-propanol and hydrogen partial pressures on the overall kinetics.

Our goal was to determine the optimum catalyst metal loading and acid–base properties required for the MIBK synthesis as well as the most favorable reaction conditions for improving the MIBK yield. Results show that a low-copper loading Cu–Mg–Al catalyst operating in the gas-phase at atmospheric pressure, relatively high temperatures and inert atmosphere gives MIBK yields similar to that of the industrial process from DMK at high pressures. Furthermore, the MIBK yield can be improved further by increasing the 2-propanol partial pressure in the feed.

2. Experimental

2.1. Catalyst preparation

Catalyst precursors of Cu-containing $\text{CuM}_I(\text{M}_{II})\text{O}_x$ mixed oxides, where M_I and M_{II} are metal cations like Mg^{2+} , Al^{3+} or Ce^{3+} , were prepared by coprecipitation following similar procedures. An aqueous solution of the metal nitrates with a total $[\text{Cu}^{2+} + \text{M}_I + \text{M}_{II}]$ cation concentration of 1.5 M was contacted with an aqueous solution of KOH and K_2CO_3 at a constant pH of 10. Both solutions were simultaneously added dropwise to 300 mL of distilled water kept at 338 K in a stirred batch reactor. The resulting precipitates were aged for 2 h at 338 K in their mother liquor and then filtered, washed thoroughly with 900 mL of deionized water at 373 K, and finally dried at 393 K overnight. Dried precipitates were decomposed overnight in air at 723–773 K in order to obtain the corresponding mixed oxides.

2.2. Catalyst characterization

The crystalline phases in the coprecipitates and in the mixed oxides were determined by X-ray diffraction (XRD) using a

Shimadzu XD-D1 diffractometer and Ni-filtered Cu K α radiation.

CO₂ adsorption site densities (n_b) and binding energies were obtained from temperature-programmed desorption (TPD) of CO₂ pre-adsorbed at room temperature. Samples (150 mg) were pre-treated in N₂ at 773 K for 1 h and then exposed to a flow of 3% CO₂/N₂ at room temperature for 0.08 h. Weakly adsorbed CO₂ was removed by flowing 50 cm³/min of N₂ and then the temperature was increased to 773 K at 10 K/min. Desorbed CO₂ was converted in CH₄ on a methanation catalyst (Ni/Kieselghur) and then analyzed using a flame ionization detector.

The structure of CO₂ chemisorbed on the mixed oxide samples was determined by infrared spectroscopy (IR). Data were obtained using a Shimadzu FTIR-8101M spectrophotometer after admission of 5.3 kPa of CO₂, adsorption at room temperature and sequential evacuation at 298, 373, 473, and 573 K. Spectra were taken at room temperature. An inverted T-shaped Pyrex cell containing the sample pellet was used. The two ends of the short arm of the T were fitted with CaF₂ windows. The absorbance scales were normalized to 50 mg pellets.

Acid site densities (n_a) were determined by TPD of NH₃ pre-adsorbed at room temperature. Samples (100 mg) were pre-treated in He at 773 K for 1 h and then exposed at room temperature to a flow of 1.01% NH₃/He until surface saturation. Weakly adsorbed NH₃ was removed by flowing 60 cm³/min of He and then the temperature was increased to 773 K at 10 K/min. The NH₃ concentration in the effluent was analyzed by mass spectrometry (MS).

BET surface areas (S_g) were measured by N₂ physisorption at its boiling point using a Quantachrome Nova-1000 sorptometer. Copper and residual potassium contents of the samples were determined by atomic absorption spectroscopy (AAS).

The dispersion of the metallic copper particles, defined as the ratio of the number of surface metallic copper atoms (Cu⁰)_s to the total copper atoms in the catalyst formulation, was determined by titration with N₂O at 363 K using a stoichiometry of (Cu⁰)_s/N₂O = 2 [21]. Pre-reduced samples were exposed to pulses of N₂O in a flow of He. The number of chemisorbed oxygen atoms was calculated from the consumption of N₂O measured by MS.

2.3. Catalytic testing

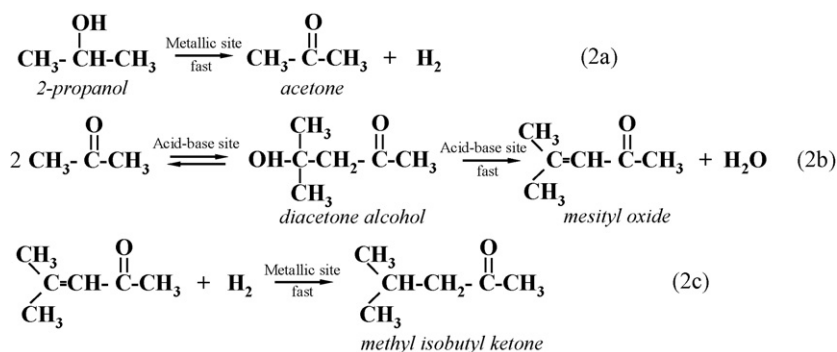
Catalytic tests were conducted at 453–533 K and atmospheric pressure in a fixed bed reactor. Samples sieved at 0.35–0.42 mm were pre-treated in N₂ at 773 K for 1 h before reaction in order to remove adsorbed H₂O and CO₂. Then, catalysts were reduced in situ in flowing H₂ at 573 K for 1 h prior the catalytic test.

The reactant, 2-propanol (Merck, ACS, 99.5% purity) was introduced via a syringe pump and vaporized into flowing N₂, H₂ or a mixture of both to give 2-propanol partial pressures in the range of 3.0–38.0 kPa. Reaction products were analyzed by on-line gas chromatography using an ATI Unicam 610 chromatograph equipped with a flame ionization detector and a 0.2% Carbowax 1500/80–100 Carbowax C column. Data were collected every 1 h for 6 h. Main reaction products were identified as propane (C₃), DMK, MIBK, and methyl isobutyl carbinol (MIBC). At high conversion levels di-isobutyl ketone (DIBK), di-isobutyl carbinol (DIBC) and other unidentified heavy condensation products were also obtained. Due to a slight catalyst deactivation process, the catalytic results reported here were calculated by extrapolation of the reactant and product concentration curves to zero time on stream. Then, X , η and S represent conversion, yield and selectivity at $t = 0$, respectively.

3. Results and discussion

3.1. Reaction network and preliminary catalyst selection for MIBK synthesis

The synthesis of MIBK from 2-propanol, Eq. (2), involves the reaction sequence depicted in Scheme 1. In the first reaction step, 2-propanol is dehydrogenated to DMK (step 2a). A catalytic formulation for MIBK synthesis must then include an active and selective metal for promoting 2-propanol dehydrogenation. In our case, we selected copper because of its known catalytic properties for the selective conversion of alcohols to carbonyl compounds such as aldehydes and ketones [22,23], and also based on our previous results. We found, in fact, that Cu/SiO₂ selectively forms DMK from 2-propanol at reaction rates up to 1000 times faster than copper-free mixed oxides [17], thereby indicating that metallic copper efficiently catalyzes alcohol dehydrogenation reactions. We also postu-



Scheme 1. Sequential reaction steps for the MIBK synthesis from 2-propanol.

lated that 2-propanol dehydrogenation on reduced copper atoms probably occurs via the formation of an alkoxide intermediate upon alcohol adsorption and further removal of the H^α in agreement with previous work on single crystals and on carbon-supported catalysts [24].

In a second reaction step, DMK is converted to MO via an aldol condensation reaction and consecutive dehydration of the aldol intermediate, diacetone alcohol (Scheme 1, step 2b). Step 2b is a sequence of elementary steps [25,26]. A surface O²⁻ Brönsted base site abstracts the α-proton of the adsorbed DMK molecule forming a carbanion intermediate, which reacts with the carbonyl group of a second DMK molecule to yield diacetone alcohol. Then, diacetone alcohol dehydrates on a surface acid site giving an α,β-unsaturated ketone, MO. The latter reaction is very rapid on mixed oxides containing acid and base sites and thus diacetone alcohol is never observed in the reaction products of the self-condensation of DMK under gas-phase reaction conditions [25]. Formation of MO from gas-phase DMK condensation is then a bimolecular reaction that requires activation of two adjacent DMK species on Brönsted base–Lewis acid pair sites. We have selected here oxides containing Mg²⁺, Ce⁴⁺ or Al³⁺ cations for promoting this reaction step, where the metal cations supply the Lewis acid site and the oxygen anions the Brönsted base site.

Finally, MO is hydrogenated to MIBK on the metallic site (Scheme 1, step 2c). The H₂ molecule generated during 2-propanol dehydrogenation (step 2a) is consumed in hydrogenating MO. Dissociative H₂ adsorption on metal atoms forms surface hydrogen fragments that hydrogenate the C=C of the MO molecule yielding the saturated ketone, MIBK. Thus, the MIBK synthesis from 2-propanol can be carried out without supplying gas-phase hydrogen in the feed.

MIBK is not a terminal product because it might be consecutively hydrogenated at the C=O bond yielding the saturated alcohol, MIBC, Eq. (3), or can further react with another DMK molecule and H₂ to yield DIBK by aldol condensation, dehydration and hydrogenation reactions, Eq. (4). DIBK might in turn be hydrogenated at the C=O bond giving the saturated alcohol, DIBC, Eq. (5).



In summary, MIBK synthesis from 2-propanol requires bifunctional catalysts that combine in intimate contact a metallic function needed for the hydro-dehydrogenation steps with an acid–base site that participates in the C=C bond forming aldol condensation reaction.

3.2. Catalyst characterization

A set of Cu-containing mixed oxides was prepared and characterized to study MIBK synthesis from 2-propanol. The physicochemical properties of these catalysts are given in Table 1. The amount of copper in all the CuM_I(M_{II})O_x samples was about 7 wt% Cu, excepting in CuMg₁₀O_x that contained 10.1 wt% Cu. The residual potassium level in all the samples was below 0.1 wt% showing that K⁺ was almost completely removed by washing the coprecipitated precursors.

XRD patterns of unreduced CuM_I(M_{II})O_x mixed oxides, Fig. 1, showed in all the cases broad XRD lines corresponding to quasi-amorphous structures, probably because the hydrated precursors were decomposed at relatively low temperatures (723–773 K). Because of the low-copper content, CuO (tenorite) was detected as an incipient and poorly crystalline phase in all the mixed oxides. Catalysts CuAl₁₆O_x and CuCe₄O_x contained single phases of γ-Al₂O₃ and CeO₂ (cerianite) while CuMg₁₀Al₇O_x and CuMg₁₀Ce₂O_x presented a MgO (periclase) phase in addition to the alumina and cerianite phases.

Dispersion of Cu⁰ particles measured by N₂O reduction was in the range of 1–14% (Table 1) in agreement with the values reported by other authors on similar low-copper loading catalysts prepared by coprecipitation [27]. Cu⁰ particle sizes of 10–100 nm were estimated from the dispersion values [28]. Ce-containing catalysts show significantly higher dispersion values attributed to a high Cu–Ce interaction [27].

The surface base properties of the CuM_I(M_{II})O_x catalysts were investigated by combining TPD and infrared measurements of CO₂ pre-adsorbed at room temperature. The surface

Table 1
Physicochemical properties of CuM_I(M_{II})O_x catalysts

Catalyst	Cu loading ^a (wt%)	Cu dispersion ^b (%)	Mg ^c (wt%)	Al ^c (wt%)	Ce ^c (wt%)	S _g ^d (m ² /g)	n _a ^e (μmol/m ²)	n _b ^f (μmol/m ²)
CuAl ₁₆ O _x	6.4	2.4	–	48.2	–	211	1.2	0.1
CuMg ₁₀ Al ₇ O _x	6.4	1.0	29.7	21.4	–	211	0.5	1.6
CuCe ₄ O _x	7.4	14.0	–	–	73.5	74	1.0	2.3
CuMg ₁₀ Ce ₂ O _x	6.9	7.0	37.0	–	30.2	102	0.3	2.7
CuMg ₁₀ O _x	10.1	N/d ^g	50.3	–	–	150	0.1	5.0

^a By AAS.

^b By N₂O chemisorption.

^c Nominal.

^d Surface area.

^e Acid site density by TPD of NH₃.

^f Base site density by TPD of CO₂.

^g Not determined

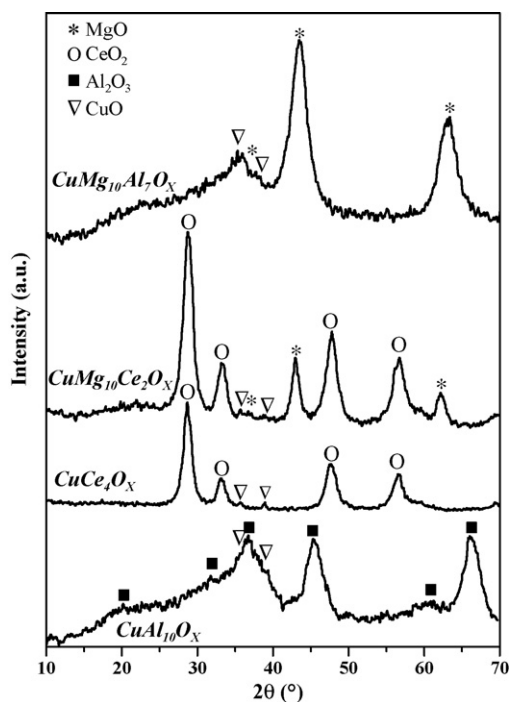


Fig. 1. XRD patterns of $\text{CuM}_I(\text{M}_{II})\text{O}_x$ mixed oxide catalysts.

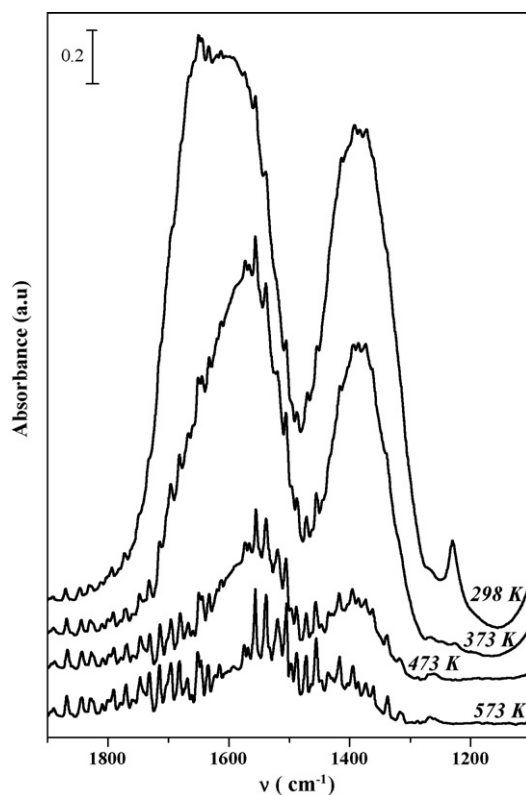


Fig. 2. IR spectra of CO_2 adsorbed at room temperature on $\text{CuMg}_{10}\text{Al}_7\text{O}_x$ (6.4 wt% Cu) and desorbed at increasing evacuation temperatures.

acid properties of the catalytic materials were determined by TPD of NH_3 pre-adsorbed at room temperature.

Total base and acid site densities (n_b) and (n_a), were calculated by integration of the CO_2 and NH_3 TPD traces (not shown). It is observed in Table 1 that the n_b values varied in a wide range ($0.1\text{--}5.0 \mu\text{mol CO}_2/\text{m}^2$) whereas the n_a values varied in a narrower range between 0.1 and $1.2 \mu\text{mol NH}_3/\text{m}^2$. The n_b and n_a values depended on the acid–base properties of metal cations M_I and M_{II} , so that oxides containing more electronegative cations (Lewis acids) such as Al^{3+} in $\text{CuAl}_{16}\text{O}_x$ present moderate density of acid sites and low density of base sites. Contrarily, oxides of less electronegative cations such as Mg^{2+} in $\text{CuMg}_{10}\text{O}_x$ show a high base site density and poor acidic features.

In previous work [29,30], we characterized the surface basicity of different copper-free Mg-based oxides and identified by FTIR of CO_2 three different CO_2 surface species formed on oxygen sites of different chemical environment. Unidentate carbonate forms on low-coordination surface O^{2-} ions such as those present in corners or edges and exhibits a symmetric O–C–O stretching at $1360\text{--}1400 \text{ cm}^{-1}$ and an asymmetric O–C–O stretching at $1510\text{--}1560 \text{ cm}^{-1}$. Bidentate carbonate forms on Lewis acid–Brønsted base pairs ($\text{M}^{n+}\text{--O}^{2-}$ pair site, where M^{n+} is the metal cation) and shows a symmetric O–C–O stretching at $1320\text{--}1340 \text{ cm}^{-1}$ and an asymmetric O–C–O stretching at $1610\text{--}1630 \text{ cm}^{-1}$. Bicarbonate species formation involves surface hydroxyl groups and shows a C–OH bending mode at 1220 cm^{-1} as well as symmetric and asymmetric O–C–O stretching bands at 1480 cm^{-1} and 1650 cm^{-1} , respectively [31–33]. We also determined the following base strength order for these surface oxygen species: low-coordination O^{2-}

anions greater than oxygen in $\text{M}^{n+}\text{--O}^{2-}$ pairs and greater than OH groups [29,30].

Similarly, the structure of the chemisorbed CO_2 species on unreduced catalyst $\text{CuMg}_{10}\text{Al}_7\text{O}_x$ was determined here by FTIR after CO_2 adsorption at room temperature and sequential evacuation at 298, 373, 473 and 573 K, Fig. 2. The spectra of Fig. 2 show the same CO_2 surface species and binding energies previously found on copper-free mixed oxides. In fact, bicarbonate bands disappeared following evacuation at 373 K indicating that the surface OH groups are weak base sites whereas unidentate and bidentate carbonates remained on the surface even after evacuation at 473 K, reflecting their stronger basicity. After evacuation at 573 K only the bands of unidentate species were detected, thereby revealing that the basic strength of low-coordination O^{2-} sites is higher than that of oxygen in $\text{M}^{n+}\text{--O}^{2-}$ pairs.

The binding energies of CO_2 on the $\text{CuM}_I(\text{M}_{II})\text{O}_x$ catalysts of Table 1 were compared by measuring the CO_2 desorption peak temperatures in the respective TPD curves. We found that the CO_2 desorption temperatures are strongly related to the electronegativity of the metal cations. Thus, the Al^{3+} cations in $\text{CuAl}_{16}\text{O}_x$ give rise to the weakest base sites (CO_2 desorption temperature $\approx 350 \text{ K}$), whereas Ce^{4+} in CuCe_4O_x introduces low- ($\approx 400 \text{ K}$) and medium-strength ($\approx 500 \text{ K}$) base sites. The Mg-containing samples ($\text{CuMg}_{10}\text{Al}_7\text{O}_x$, $\text{CuMg}_{10}\text{Ce}_2\text{O}_x$, $\text{CuMg}_{10}\text{O}_x$) presented not only weak and medium-strength base sites but also strong base sites, as indicated by the presence of high-temperature desorption peaks ($\approx 550 \text{ K}$). By deconvolution of the CO_2 TPD profiles, it was found that the contribution of the

high-temperature peak to the total base site density increased with the Mg content in the sample, thereby showing that the Mg^{2+} cations generate surface oxygen anions that strongly bind CO_2 . The area of the high-temperature peak represented 58% of the total area in the CO_2 TPD trace of $\text{CuMg}_{10}\text{O}_x$, the sample containing the highest Mg loading (Table 1).

The NH_3 binding energies, on the other hand, seem not to be significantly affected by the catalyst chemical composition since the NH_3 TPD profiles for all the $\text{CuM}_1(\text{M}_{\text{II}})\text{O}_x$ catalysts present a broad desorption peak at about 450–500 K attributed to H-bonded adsorption on weak Brønsted sites (OH groups) overlapping the irreversible NH_3 coordination to Lewis acid cations of moderate strength [34]. This result is probably due to the fact that none of the catalysts contains strong Lewis acid cations or strong protons (Brønsted acid sites).

3.3. Catalytic results

3.3.1. Effect of the catalyst acid–base properties

As depicted in Scheme 1, the catalyst acid–base properties are expected to affect the C=C bond forming aldol condensation reaction. The effect of the acid–base properties on MIBK synthesis was analyzed here by comparing the catalytic performance of $\text{CuM}_1(\text{M}_{\text{II}})\text{O}_x$ samples at $\sim 40\%$ conversion and 473 K, in H_2 atmosphere. Results are presented in Fig. 3. A contact time (W/F^0) of 3.6 g cat. h/mol was used with all the catalysts of Fig. 3 except with $\text{CuMg}_{10}\text{Al}_7\text{O}_x$ that was more active and required a W/F^0 of 1.2 g cat. h/mol to convert 40% of 2-propanol.

MO, the α,β -unsaturated C_6 intermediate was not observed in any of the experiments of Fig. 3. At 40% 2-propanol conversion, MIBK was obtained with higher selectivities than the saturated alcohol MIBC or the consecutive aldol condensation product DIBK on all the catalysts except CuCe_4O_x .

The selectivity to C_6 aldol condensation products (MIBK and MIBC) on $\text{CuAl}_{16}\text{O}_x$ was very low, about 3%, thereby

indicating that DMK condensation to MO is poorly promoted on this sample. Furthermore, $\text{CuAl}_{16}\text{O}_x$ produced 2% of propane (C_3), an undesirable by-product formed from 2-propanol dehydration on acid sites. This result would reflect the Lewis acidic features of the Al^{3+} cations and the relatively large number of acid sites present on this sample (Table 1). It seems then that acidic catalysts with low density of base sites such as $\text{CuAl}_{16}\text{O}_x$ are not able to efficiently promote the aldol condensation of DMK to MO.

When a less electronegative cation such as Mg^{2+} or Ce^{4+} was included in the catalyst formulation (samples $\text{CuMg}_{10}\text{Ce}_2\text{O}_x$ and $\text{CuMg}_{10}\text{O}_x$), the selectivity to C_3 was negligible and the selectivity to C_6 aldol condensation compounds was about 10–13%, significantly higher than the selectivity value obtained on $\text{CuAl}_{16}\text{O}_x$. This selectivity improvement to the formation of MIBK and MIBC is explained by considering the higher density of base sites and lower density of acid sites present on Mg- and Ce-containing oxides compared to $\text{CuAl}_{16}\text{O}_x$. Catalysts $\text{CuMg}_{10}\text{Ce}_2\text{O}_x$ and $\text{CuMg}_{10}\text{O}_x$, in fact, have the highest total base site densities (n_b , Table 1) and contain a high proportion of strong base sites not present in the other catalysts.

But the most selective catalysts for the formation of MIBK and MIBC were CuCe_4O_x and $\text{CuMg}_{10}\text{Al}_7\text{O}_x$ that present both a moderate density of acid and base sites. The selectivity to C_6 aldol condensation compounds on these catalysts reached about 20% (Fig. 3). It appears that the C=C bond forming reaction is preferentially promoted on catalysts containing weak Lewis acid cations such as Ce^{4+} or a proper combination of Mg^{2+} – Al^{3+} cations. Nevertheless, although the MIBK formation rate was similar on CuCe_4O_x and $\text{CuMg}_{10}\text{Al}_7\text{O}_x$ the activity decay on stream was faster on the former, probably because of the formation of higher amounts of heavy C_{9+} compounds (Fig. 3). Thus, we selected $\text{CuMg}_{10}\text{Al}_7\text{O}_x$ as the most promising catalyst to continue our investigations on MIBK synthesis from 2-propanol.

3.3.2. Effect of the copper content

In previous studies on MIBK synthesis by the conventional DMK + H_2 process, it was found that there is an optimum metal content because, in general, DMK conversion increases but MIBK selectivity decreases with increasing the metal loading [4,11,35,36]. The metal content is expected to influence the MIBK synthesis from 2-propanol too, because the first and the last reaction steps in Scheme 1 are promoted by metallic sites. Therefore, we investigated here the effect of Cu loading on the catalyst activity and selectivity using the previously selected $\text{CuMg}_{10}\text{Al}_7\text{O}_x$ catalyst that contains a Mg/Al molar ratio of 1.4. The copper content was varied between 0.27 and 6.4 wt%, whereas the Mg/Al ratio was maintained constant. These materials are referred to as $\text{Cu}_z\text{Mg}_{10}\text{Al}_7\text{O}_x$ oxides.

The copper loading did not significantly affect the surface areas of the $\text{Cu}_z\text{Mg}_{10}\text{Al}_7\text{O}_x$ oxides which were between 211 and 260 m^2/g . Similarly, the n_b values measured by TPD of CO_2 were almost independent of the Cu concentration. The CO_2 binding energies on the different $\text{Cu}_z\text{Mg}_{10}\text{Al}_7\text{O}_x$ oxides were comparable to those of catalyst $\text{CuMg}_{10}\text{Al}_7\text{O}_x$ (6.4 wt% Cu), with the main CO_2 desorption peak at 400 K. Therefore, base

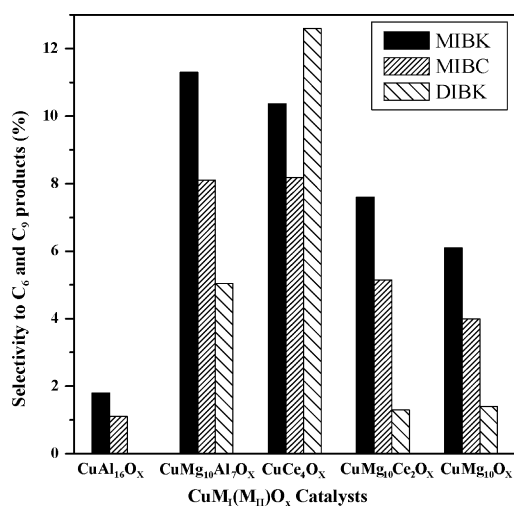


Fig. 3. MIBK synthesis from 2-propanol: selectivity to C_6 and C_9 products on $\text{CuM}_1(\text{M}_{\text{II}})\text{O}_x$ mixed oxide catalysts [$T = 473$ K; $P_T = 101.3$ kPa; $P_{2\text{-propanol}}^0 = 7.8$ kPa; H_2 balance; $X_{2\text{-propanol}} = 40\%$].

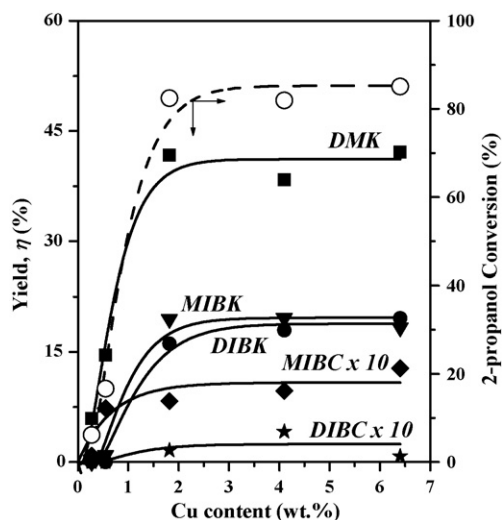


Fig. 4. Effect of Cu loading on catalytic performance of $\text{Cu}_z\text{Mg}_{10}\text{Al}_7\text{O}_x$ mixed oxide catalysts [$T = 473\text{ K}$; $P_T = 101.3\text{ kPa}$; $W/F^0 = 3.6\text{ g h/mol}$, $P_{2\text{-propanol}}^0 = 7.8\text{ kPa}$, N_2 balance].

site density and strength distribution were not much affected by the copper content.

The catalytic results obtained on $\text{Cu}_z\text{Mg}_{10}\text{Al}_7\text{O}_x$ oxides at 473 K in N_2 atmosphere are presented in Fig. 4. 2-propanol conversion increased from 6 to 82% when the Cu content was augmented from 0.27 to 1.82 wt% and then remained almost constant for higher Cu concentrations.

It seems that in low-metal loading catalysts (our samples containing 0.27 and 0.55 wt% Cu) copper is excessively diluted and buried inside the mixed oxide matrix to perform the dissociative 2-propanol adsorption leading to DMK at high rates. Similarly, Barth et al. [37] reported that Co/SiO_2 catalysts with cobalt loadings below 0.4 wt% were inactive for 2-propanol dehydrogenation. They attributed this result to irreducibility of cobalt ions due to a metal-support interaction. We made an attempt to measure the copper dispersion on the catalysts containing 0.27 and 0.55 wt% Cu, but we did not detect any N_2O decomposition. Consistently, Kenvin and White [38] observed that low-metal Cu/SiO_2 samples do not react with N_2O . They explained this result by considering that low-copper loading catalysts do not have copper atoms close enough to form the ensembles required to decompose N_2O . The linear dependence observed in Fig. 4 between 2-propanol conversion and copper content for low-metal loading catalysts probably reflects the increase of the kinetic constant of the 2-propanol dehydrogenation reaction which is promoted on metallic sites. In other words, DMK formation would be the rate determining step for low values of 2-propanol conversion as it is suggested by the DMK selectivities of 90–95% measured from the results of Fig. 4 on catalysts containing 0.27 and 0.55 wt% Cu.

By increasing the copper loading up to about 2%, the catalyst activity increases but the selectivity to DMK concomitantly decreases because the formation of consecutive C_6 and C_9 products by aldol condensation takes place at increasing rate. For higher Cu loadings both 2-propanol conversion and product yields level off because the reaction

kinetics is now controlled by the aldol condensation reaction that is not promoted on metallic sites. It is worth noting that also the catalyst activity decay was similar on samples containing less or equal to 1.82 wt% Cu. We observed, in fact, that the samples with 1.82, 4.1 and 6.4% Cu lost about 10% activity after the 6-h catalytic run.

In summary, our catalytic results show that the Cu content can be decreased to about 2 wt% without causing significant changes on the catalyst activity, selectivity and stability.

3.3.3. Effect of the reaction temperature

The conventional MIBK synthesis from $\text{DMK} + \text{H}_2$, Eq. (1), must be carried out at low temperatures (393–433 K) because of thermodynamic constraints derived from the fact that the overall reaction is strongly exothermic (-22.5 kcal/mol at 393 K). Contrarily, our calculations for Eq. (2) using additivity rules for the estimation of thermodynamic parameters [39] indicate that 2-propanol equilibrium conversion is around 100% for reaction temperatures in the range of 300–600 K, thereby confirming the absence of thermodynamic limitations for the MIBK synthesis from 2-propanol.

Furthermore, our calculations led us to conclude that the gas-phase MIBK synthesis reaction from 2-propanol is a slightly endothermic process (0.7 kcal/mol at 473 K). Therefore, the increase of the reaction temperature is expected to improve the MIBK formation rate but not to influence significantly the thermodynamics of the overall MIBK synthesis process. However, the effect of the reaction temperature will be important on the thermodynamics of each individual reaction involved in the MIBK synthesis process, i.e., the three steps of Eq. (2), and Eqs. (3)–(5), by modifying the product distribution at each reaction temperature.

The effect of temperature on the catalytic performance of $\text{CuMg}_{10}\text{Al}_7\text{O}_x$ (6.4 wt% Cu) was investigated in the range of 453–533 K and in the absence of gas-phase hydrogen in the feed, i.e., 2-propanol was vaporized in a N_2 flow. Results are shown in Fig. 5A. As expected, conversion increased with increasing temperature and a 2-propanol conversion of 95% was obtained at 533 K.

The DMK yield increased with temperature and then reached a maximum at about 513 K while the MIBK formation augmented monotonically with temperature. This result shows that at high temperatures the consecutive transformation of DMK to MO (step 2b, Scheme 1) predominates over DMK formation, thereby suggesting that on $\text{CuMg}_{10}\text{Al}_7\text{O}_x$ the apparent activation energy of the self-condensation of DMK is higher than that of 2-propanol dehydrogenation. Both reactions are endothermic and are not limited by equilibrium under our reaction conditions.

At a reaction temperature of 533 K η_{MIBK} reached a value of 27%; this value is comparable to the 30% of the current commercial MIBK synthesis process from DMK at high pressures. On the other hand, it appears that hydrogenation of the $\text{C}=\text{C}$ of MO to MIBK (step 2c, Scheme 1) takes place much faster than MO desorption because only traces of gaseous MO were detected on our copper catalyst, even at high conversion levels (Fig. 5A).

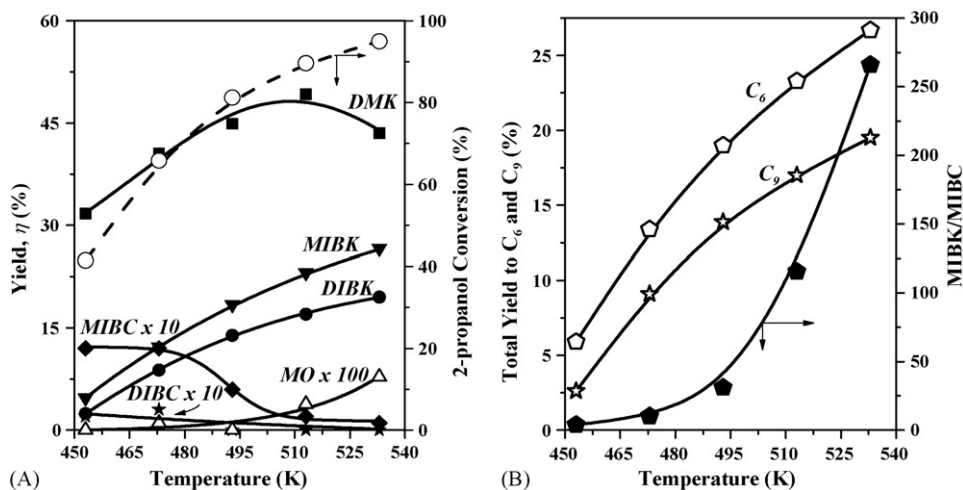


Fig. 5. Effect of the reaction temperature on the catalytic performance of $\text{CuMg}_{10}\text{Al}_7\text{O}_x$ (6.4% Cu) [$W/F^0 = 2.8$ g h/mol; $P_T = 101.3$ kPa; $P_{2\text{-propanol}}^0 = 7.8$ kPa, N_2 balance].

Formation of MIBK and DIBK by hydrogenation of MIBK and DIBK, Eqs. (3) and (5), respectively, are exothermic reactions severely limited by the thermodynamics. This explains that η_{MIBK} and η_{DIBK} decreased with temperature in Fig. 5A. As a consequence of the opposite trend observed for MIBK and MIBC yields with temperature, the MIBK/MIBC ratio is drastically improved by increasing the reaction temperature, as it is shown in Fig. 5B.

The increase of η_{DIBK} with temperature follows that of MIBK in Fig. 5A because DIBK is formed by aldol condensation of MIBK with DMK, Eq. (4). The total yield to C₆ products (MIBK + MIBC) was higher than that of C₉ compounds (DIBK + DIBC) at all the reaction temperatures of this study (Fig. 5B).

Finally, we remark that formation of C₃ was negligible (<0.05%) even at high temperatures. This shows that the undesirable 2-propanol dehydration, which is an endothermic reaction, is not kinetically significant on the basic $\text{CuMg}_{10}\text{Al}_7\text{O}_x$ catalyst.

Catalyst stability was slightly decreased by increasing the reaction temperature. At 533 K, catalyst $\text{CuMg}_{10}\text{Al}_7\text{O}_x$ (6.4 wt% Cu) lost about 20% activity after the 6-h catalytic run due to formation of high boiling point C₉₊ oxygenates, whereas at 453–473 K the deactivation was negligible. Sintering of the metal particles is not likely to contribute to the deactivation process at high temperatures because of the low surface hydrogen pressure in the catalytic experiments and because the catalyst was previously treated with pure hydrogen at a temperature higher than that of the catalytic runs (573 K).

3.3.4. Effect of the 2-propanol partial pressure

The effect of the reactant composition in the feed was investigated on catalyst $\text{CuMg}_{10}\text{Al}_7\text{O}_x$ (6.4 wt% Cu) at 473 K and at a contact time of 0.48 g cat. h/mol in a wide 2-propanol partial pressure range of 3.0–38.0 kPa. A low contact time value was chosen for these experiments in order to keep the 2-propanol conversion around 20–25%. Results are presented in Fig. 6.

The catalyst activity increased with 2-propanol partial pressure in the entire $P_{2\text{-propanol}}^0$ range studied. By plotting 2-propanol conversion rate as a function of $P_{2\text{-propanol}}^0$ in logarithmic scale we obtained a straight line. From the slope of this plot we calculated an apparent 2-propanol reaction order of 0.17 on the overall kinetics. Rioux and Vannice [28] studied the kinetics of 2-propanol dehydrogenation to DMK, step 2a, on carbon-supported Cu catalysts and postulated a Langmuir–Hinshelwood–Hougen–Watson (L–H–H–W) surface reaction mechanism consistent with a reaction order in 2-propanol of 0.34 at 473 K for 2-propanol partial pressures of up to 7.0 kPa.

The formation rate of MIBK and other products also increased by increasing the 2-propanol partial pressure (Fig. 6). In particular, a 10-fold increase of the 2-propanol partial pressure, increased the MIBK formation rate by a factor of 2. From the values of Fig. 6, we calculated an apparent order in 2-propanol of 0.35 for the MIBK formation rate. This value is in agreement with the results reported by Melo et al. [40]. These authors investigated the kinetics of the gas-phase MIBK

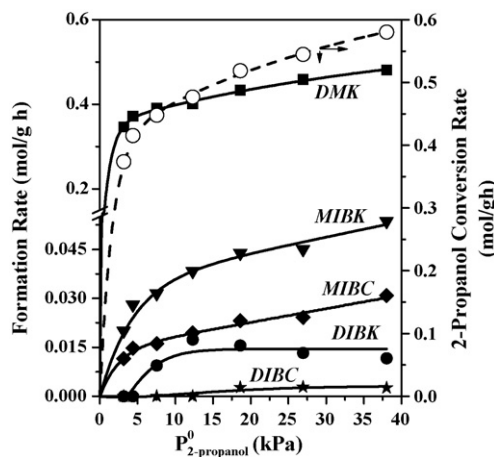


Fig. 6. Effect of the 2-propanol partial pressure on the catalytic performance of $\text{CuMg}_{10}\text{Al}_7\text{O}_x$ (6.4% Cu) [$W/F^0 = 0.48$ g h/mol; $T = 473$ K; $P_T = 101.3$ kPa; $P_{\text{H}_2}^0 = 39.6$ kPa, N_2 balance].

synthesis by the conventional technology from DMK, Eq. (1) on Pt/HZSM5, at 463 K and atmospheric pressure, and found that the apparent order with respect to DMK was 0.3 for the MIBK formation rate.

3.3.5. Effect of the hydrogen partial pressure

In a previous work [17], we investigated the reaction pathways leading from 2-propanol to MIBK and other products by varying the contact time (W/F^0) in different reaction atmospheres (with or without supplying gas-phase hydrogen) at 473 K. The results suggested that the same reaction pathways leading to MIBK, MIBC and DIBK apply in both atmospheres. However, when the reaction was carried out in N_2 , 2-propanol conversions were higher than in H_2 what indicates that gaseous hydrogen is detrimental to the catalytic activity.

Here, we have investigated further the influence of hydrogen on the catalytic performance of sample $CuMg_{10}Al_7O_x$ (6.4 wt% Cu) at 473 K and at a low contact time of 0.48 g cat. h/mol, by systematically varying the hydrogen partial pressure between 0.0 and 94.0 kPa while maintaining constant the 2-propanol pressure at 7.8 kPa. Results are presented in Fig. 7. Thermodynamic calculations for Eq. (2) indicate that the 2-propanol equilibrium conversion at 473 K is around 100% regardless of the hydrogen partial pressure, and consequently a thermodynamic hindrance has to be ruled out when interpreting the results of Fig. 7.

The catalyst activity remained practically constant when the H_2 partial pressure was increased up to about 50 kPa but higher H_2 pressures decreased the 2-propanol conversion rate. Our results obtained in the low H_2 partial pressure region are in agreement with those reported by Roix and Vannice [28,41]. These authors, in fact, studied the gas-phase 2-propanol dehydrogenation to DMK (step 2a) on carbon-supported Cu catalysts and found a near zero-order dependency in hydrogen when exploring hydrogen pressures of up to 23 kPa at 473 K.

The effect of $P_{H_2}^0$ on the MIBK formation rate was qualitatively similar to that found for DMK, i.e., the use of high H_2 pressures inhibited the MIBK synthesis. This result may be

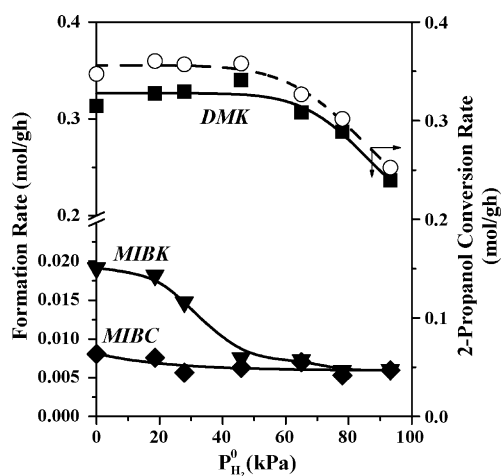


Fig. 7. Effect of the H_2 partial pressure on the catalytic performance of $CuMg_{10}Al_7O_x$ (6.4% Cu) [$W/F^0 = 0.48$ g h/mol; $T = 473$ K; $P_T = 101.3$ kPa; $P_{2-propanol}^0 = 7.8$ kPa, N_2 balance].

explained by considering that the MIBK formation kinetics is essentially determined by the MO formation rate from aldol condensation of DMK (Scheme 1, step 2b), the consecutive MO hydrogenation to MIBK not being kinetically significant. The rapid MO transformation to MIBK is in agreement with the fact that the MO concentration detected in gas-phase was negligible. From the values of Fig. 7 for hydrogen partial pressures less or equal to 18 kPa we calculated an apparent H_2 negative reaction order of -0.74 on the MIBK formation rate consistently with the fact that H_2 is a product of the MIBK synthesis from 2-propanol. On the contrary, results in literature show that the MIBK formation from DMK is favored by increasing the H_2 pressure. For example, Melo et al. [40] studied the kinetics of the gas-phase MIBK synthesis from DMK on Pt/HZSM5 and reported an apparent reaction order in hydrogen of 1.3 for hydrogen partial pressures of up to 80 kPa. Similarly, ÓKeefe et al. [42] investigated the liquid-phase formation of MIBK from MO (Scheme 1, step 2c) on Pd/ Al_2O_3 at 373 K and found that the reaction is first order with respect to hydrogen for partial pressures of 1.5–4.23 MPa. The results reported in these two papers are in agreement with the fact that hydrogen is a reactant in both step 2c and Eq. (1).

The MIBC formation rate did not change by varying $P_{H_2}^0$ (Fig. 7). This result suggests that MIBC is not formed by any reaction requiring the presence of molecular H_2 in gas-phase, and is consistent with the fact that the MIBK hydrogenation to MIBC is severely limited by thermodynamics. Thus, MIBC would be mainly formed via a hydrogen transfer reaction between MO and 2-propanol, acting 2-propanol as the hydrogen donor molecule. As we have reported [43], this reaction does not require the presence of gas-phase H_2 to proceed and is promoted on oxides containing a high density of acid–base pair sites.

4. Conclusions

The one-step synthesis of MIBK from 2-propanol is satisfactory carried out at mild temperatures and atmospheric pressure on a $Cu_zMg_{10}Al_7O_x$ bifunctional catalyst that combines in intimate contact the metallic function (Cu^0) required for hydro-dehydrogenation steps and the acid–base pair sites needed for the C=C bond forming aldol condensation reaction leading from DMK to MIBK. The copper loading can be varied between 2 and 6 wt% without affecting the catalyst activity, selectivity and stability.

Conversion of 2-propanol significantly increases with temperature and values of 90–100% can be reached at about 533 K and reasonable low contact times. The yield to MIBK also augments monotonically with temperature while the DMK formation increases initially but then reaches a maximum at about 513 K, probably reflecting that on $CuMg_{10}Al_7O_x$ catalyst the apparent activation energy of the self-condensation of DMK is higher than that of 2-propanol dehydrogenation. The consecutive hydrogenation of MIBK to MIBC is an exothermic reaction severely limited by thermodynamics that causes the diminution of MIBC yield when increasing the temperature. In contrast, formation DIBK from the aldol condensation of

MIBK with DMK increases with temperature because the reaction has not thermodynamic constraints.

The catalyst activity and MIBK formation rate diminish with increasing the H₂ partial pressure, which reflects a negative order with respect to H₂ in the reaction kinetics. Contrarily, the MIBK formation rate can be improved by increasing the 2-propanol partial pressure in the feed because the reaction is positive reaction order with respect to 2-propanol.

On CuMg₁₀Al₇O_x, operation at 533 K and atmospheric pressure yielded 27% of MIBK among other valuable oxygenates such as DMK and DIBK. This promising value is close to the 30% MIBK yield of the current commercial process from DMK carried out in liquid-phase at high pressures.

Acknowledgements

Authors thank the Universidad Nacional del Litoral (UNL), Santa Fe and the Agencia Nacional de Promoción Científica y Tecnológica (ANPCyT), Argentina for the financial support of this work (grant PICTO 13234 BID 1728/OC-AR). The authors also thank H. Cabral for technical assistance.

References

- [1] Ullmann's Encyclopedia of Industrial Chemistry, sixth ed., in CD ROM, 2002.
- [2] W. Reith, M. Detmer, H. Widdecke, B. Fleischer, in: M. Guisnet, et al. (Eds.), *Heterogeneous Catalysis and Fine Chemicals II*, Elsevier, Amsterdam, 1991.
- [3] A. Mitschker, R. Wagner, P.M. Lange, in: M. Guisnet, et al. (Eds.), *Heterogeneous Catalysis and Fine Chemicals I*, Elsevier, Amsterdam, 1988, p. 61.
- [4] Y.Z. Chen, C.M. Hwang, C.W. Liaw, *Appl. Catal. A: Gen.* 169 (1998) 207.
- [5] S. Talwalkar, S. Mahajani, *Appl. Catal. A: Gen.* 302 (2006) 140.
- [6] C. Hakuu, S. Koyou, C. Yoshimasa, C. Nansei, H. Bunki, S. Sokon, Japanese Patent 2,069,430 (1990).
- [7] E.F. Kozhevnikova, I.V. Kozhevnikov, *J. Catal.* 238 (2006) 286.
- [8] M.J. Martinez-Ortiz, D. Tichit, P. Gonzalez, B. Coq, *J. Mol. Catal. A: Chem.* 201 (2003) 199.
- [9] R. Unnikrishnan, S.J. Narayanan, *J. Mol. Catal. A: Chem.* 144 (1999) 173.
- [10] S. Narayanan, R. Unnikrishnan, *Appl. Catal. A: Gen.* 145 (1996) 231.
- [11] V. Chikan, A. Molnar, K. Balazsik, *J. Catal.* 184 (1999) 134.
- [12] A. Molnar, M. Varga, G. Mulas, M. Mohai, I. Bertoti, A. Lovas, G. Cocco, *Mater. Sci. Eng. A* 304–306 (2001) 1078.
- [13] K. Weissmermel, H.-J. Arpe, *Industrial Organic Chemistry*, fourth ed., Wiley-VCH, Weinheim, 2003.
- [14] H.R. Arnold, US Patent 2,046,145 (1936).
- [15] D.K. MacAlpine, B.L. Williams, P.S. Williams, *European Patent Appl.* 188,899A1 (1986).
- [16] H. Zdenek, Z. Rudolf, K. Jiri, CS Patent 241,425 (1986).
- [17] J.I. Di Cosimo, G. Torres, C.R. Apesteguía, *J. Catal.* 208 (2002) 114.
- [18] J.I. Di Cosimo, A. Acosta, C.R. Apesteguía, *J. Mol. Catal. A: Chem.* 222 (2004) 87.
- [19] T.M. Jyothi, T. Raja, B.S. Rao, *J. Mol. Catal. A: Chem.* 168 (2001) 187.
- [20] M.A. Aramendía, V. Borau, C. Jiménez, J.M. Marinas, A. Porras, F.J. Urbano, *Appl. Catal. A: Gen.* 172 (1998) 31.
- [21] A. Dandekar, M.A. Vannice, *J. Catal.* 178 (1998) 621.
- [22] M. Kraus, in: G. Ertl, et al. (Eds.), *Handbook of Heterogeneous Catalysis*, Wiley-VCH, Weinheim, 1997.
- [23] A. Sexton, *Surf. Sci.* 88 (1979) 299.
- [24] G. Djega-Mariadassou, A.R. Marques, L. Davignon, *J. Chem. Soc. Faraday Trans. I* 78 (1982) 2447.
- [25] J.I. Di Cosimo, V.K. Díez, C.R. Apesteguía, *Appl. Catal. A: Gen.* 137 (1996) 149.
- [26] J.I. Di Cosimo, V.K. Díez, C.R. Apesteguía, *J. Appl. Clay Sci.* 13 (1998) 443.
- [27] M. Xu, M.J.L. Ginés, A.-M. Hilmen, B.L. Stephens, E. Iglesia, *J. Catal.* 171 (1997) 130.
- [28] R.M. Riuox, M.A. Vannice, *J. Catal.* 216 (2003) 362.
- [29] V.K. Díez, C.R. Apesteguía, J.I. Di Cosimo, *J. Catal.* 240 (2006) 235.
- [30] J.I. Di Cosimo, V.K. Díez, M. Xu, E. Iglesia, C.R. Apesteguía, *J. Catal.* 178 (1998) 499.
- [31] R. Philipp, K. Fujimoto, *J. Phys. Chem.* 96 (1992) 9035.
- [32] C. Morterra, G. Ghiotti, F. Boccuzzi, S. Coluccia, *J. Catal.* 51 (1978) 299.
- [33] T. Kanno, M. Kobayashi, in: M. Misono, Y. Ono (Eds.), *Acid-Base Catalysts II*, Elsevier, Kodansha, 1994.
- [34] V.K. Díez, C.R. Apesteguía, J.I. Di Cosimo, *J. Catal.* 215 (2003) 220.
- [35] N. Cheiki, M. Kacimi, M. Rouimi, M. Ziyad, L.F. Liotta, G. Pantaleo, G. Deganello, *J. Catal.* 232 (2005) 257.
- [36] S.-M. Yang, Y.M. Wu, *Appl. Catal. A: Gen.* 192 (2000) 211.
- [37] R. Barth, J.S. Falcone Jr., S. Vorce, J. McLennan, B. Outland, E. Arnoth, *Catal. Commun.* 3 (2002) 135.
- [38] J.C. Kevin, M.G. White, *J. Catal.* 130 (1991) 447.
- [39] I.M. Klotz, R.M. Rosenberg, *Chemical Thermodynamics: Basic Theory and Methods*, sixth ed., J. Wiley and Sons, New York, 2000.
- [40] L. Melo, F. Chevalier, P. Magnoux, M. Guisnet, in: *Proceedings of the XIII Iberoamerican Symposium on Catalysis*, Segovia, Spain, 1992.
- [41] R.M. Riuox, M.A. Vannice, *J. Catal.* 233 (2005) 147.
- [42] W.K. ÓKeefe, M. Jiang, F.T.T. Ng, G.L. Rempel, *Chem. Eng. Sci.* 60 (2005) 4131.
- [43] J.I. Di Cosimo, A. Acosta, C.R. Apesteguía, *J. Mol. Catal. A: Chem.* 234 (2005) 111.